Experimental Evidence for a Bragg Glass Density Wave Phase in a Transition-Metal Dichalcogenide

Jun-ichi Okamoto, Carlos J. Arguello, Ethan P. Rosenthal, Abhay N. Pasupathy, and Andrew J. Millis

Experimental evidence for a Bragg glass density wave phase in a transition-metal dichalcogenide

Jun-ichi Okamoto,* Carlos J. Arguello, Ethan P. Rosenthal, Abhay N. Pasupathy, and Andrew J. Millis

Department of Physics, Columbia University, 538 West 120th Street, New York, New York 10027, USA

(Dated: October 21, 2014)

Analysis of the spatial dependence of current-voltage characteristics obtained from scanning tunneling microscopy experiments indicates that the charge density wave (CDW) occurring in NbSe$_2$ is subject to locally strong pinning by a non-negligible density of defects, but that on the length scales accessible in this experiment the material is in a "Bragg glass" phase where dislocations and anti-dislocations occur in bound pairs and free dislocations are not observed. A Landau theory-based analysis is presented showing how a strong local modulation may produce only a weak long range effect on the CDW phase.

The effect of disorder on the properties of condensed matter systems is important both in terms of fundamental physics and of technological applications. In charge density wave (CDW) systems, randomly positioned impurities provide a random field which couples linearly to the order parameter [1]. Theory dating back to the 1970s indicates that if the impurity potential is strong enough, the random field destroys the charge density wave completely, leading to a phase with exponentially decaying correlations and a correlation length of the order of the mean distance between impurities [2, 3]. Subsequent work revised this picture, showing that in spatial dimensions $d = 3$, weak impurity pinning may lead instead to a topologically ordered "Bragg glass" phase with power-law density correlations [4–12].

While the physics of random field systems has been of intense theoretical interest, experimental information has mainly come from transport and scattering measurements which average over large sample volumes [1, 13–17]. An important exception is the flux lattice decoration experiments which provided important early support to the Bragg glass picture for vortices in superconductors [18, 19]. The development of stable scanning tunneling spectroscopy (STS) techniques which provide atomic-resolution imaging of local electronic density over wide fields of view has opened up new avenues for investigation of fundamental electronic physics, in particular providing real-space information on the effects of disorder on electronically ordered states [20, 21]. In this paper, we present an analysis of scanning tunneling spectroscopy measurements carried out on NbSe$_2$, a representative charge density wave system. The analysis motivates a Landau theory which provides insights into the effects of strong pinning in charge density wave systems.

NbSe$_2$ is a quasi-two dimensional material. Its unit cell consists of two blocks of Se-Nb-Se layers; the Nb atoms in each layer form a triangular lattice and the electrical conductivity is strongly anisotropic, being much larger for in-plane currents than for currents flowing perpendicular to the layers [22]. Scattering measurements [23]

indicate that a second order phase transition occurs at $T_c \approx 34$ K; below this temperature a charge density wave forms. The charge density wave involves condensation of electronic density at three wavevectors $\vec{Q}_{i=1,2,3}$ related by $120°$ rotations. $|\vec{Q}_i| \approx \vec{G}_i/3 \approx 0.7$ Å^{-1} with $\vec{G}_i$ the smallest nonzero reciprocal lattice vectors. We may write the modulation of the electron density $\delta\rho$ in the charge density wave phase as

$$\delta\rho(x) = \sum_{i=1}^{3} \Re\left(\psi_i(\vec{x})e^{i\vec{Q}_i \cdot \vec{x}}\right) \qquad (1)$$

The CDW order parameters ψ_i are complex numbers which may be written in terms of a real magnitude η_i and a phase ϕ_i. Deviations from perfect charge density wave order involve spatial variations of η and ϕ.

We use the scanning tunneling microscopy (STM) data shown in Fig. 1 to obtain real-space information about the spatial dependence of the amplitude $\eta(x)$ and phase $\phi(x)$. The sample used here is the one described in Ref. 24, and is made by vapor transport. The cleaved surface is believed to be a Se layer, since a Se-Se bond is van deer Waals, while a Se-Nb bond is Coulombic. Fig. 1 (a) shows the STS topographic image of the cleaved surface at 22 K $< T_c = 34$ K. The voltage and current are fixed to be -100 mV and 20 pA respectively. The measured signal is the vertical displacement of the STM tip; this depends on the physical topography and on the near Fermi-level electronic density of states at the tip position. The large number of lighter white spots form an approximately triangular lattice with mean lattice constant $\lambda \sim 1$ nm about three times the basic lattice constant, consistent with the CDW wave vector found in scattering measurements [23]. We therefore believe that these are local maxima in $\delta\rho$ arising from CDW formation. The small number of heavy white spots indicate impurities. There are about 40 impurities in this field of view, which contains $\sim 10^3$ CDW unit cells; in other words, the impurity density $n_{\text{imp}} \simeq 0.4\%$. The CDW coherence length ξ_0 is roughly of the order of the CDW period ~ 1 nm,
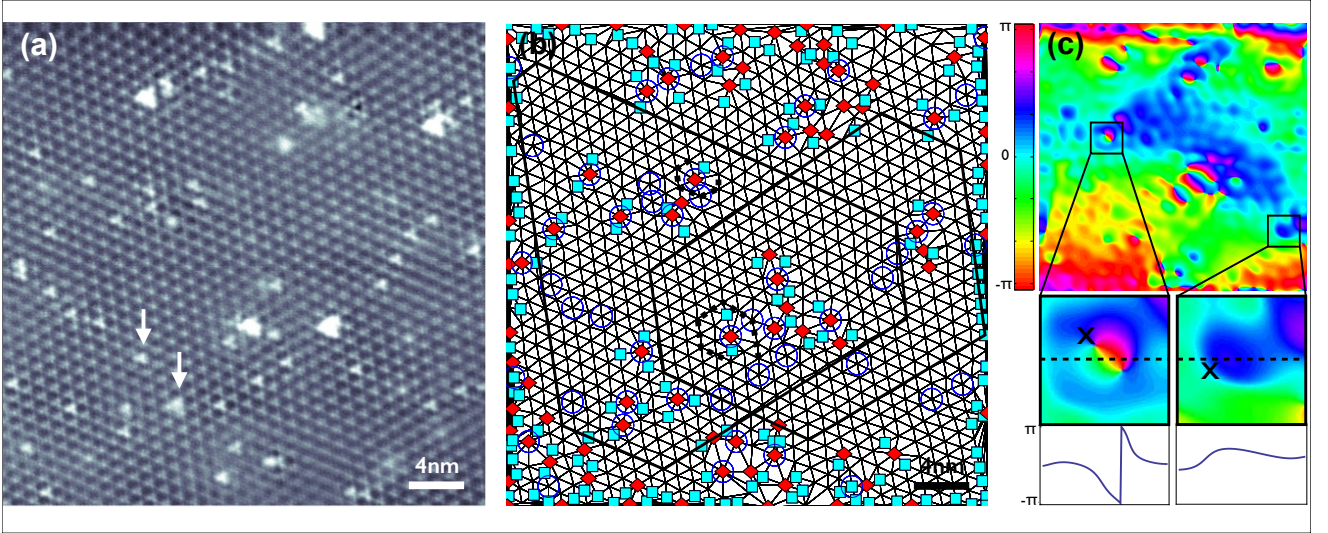
FIG. 1: (Color online) (a) A topographic image of a ~ 32 nm $\times$ 32 nm region of NbSe$_2$ at 22 K $< T_c = 34$ K taken under conditions of constant sample-tip current and bias voltage. The heavy white spots are the strong pinning centers. (b) Delaunay analysis of the image. Diamonds (squares) represent CDW maxima with more (fewer) than six edges. Impurity locations are indicated by the circles. Thick broken lines which do not close indicate that some impurities create dislocations. Larger sized thick solid loops indicate that on larger length scales there are no free dislocations. (c) Main panel is the phase configuration of the phase ϕ_1 of one of the CDW components displayed over the same field of view as shown in (a) and (b). The right inset shows a typical smooth modulation near an impurity. The left inset shows a typical vortex-antivortex pair near an impurity. X's are the locations of impurities. The lower panels of the insets are the phase profile along the dotted line.

since the phonon softening occurs over the wide range of the Brillouin zone [30, 31]. Thus, we assume that the inter-impurity distance $l \sim 5$ nm is much greater than ξ_0. The signal associated with impurities may come either from a physical change in surface height (associated e.g. with an impurity in the Se layer) or from a change in the local density of states. However, one may see that in almost all cases the impurity sits in the center of a hexagon of CDW maxima and has a triangular shape of size $\lesssim 1$ nm consistent with interference of three CDW wave vectors. This suggests that a significant contribution of the impurity signal arises from impurity-induced modulations of the density of states, and that in particular impurities lead to an increase in the local density of states which acts as a strong pinning center fixing the local CDW maximum to the impurity site. More detailed discussions about pinning are given in the supplementary material.

Fig. 2 presents the autocorrelation of the experimental signal, interpreted as a density of states modulation. We present both the density modulation relative to the average value $\delta\rho$ and the absolute value or amplitude η (the supplementary material explains how the correlation functions are defined and computed). The amplitude autocorrelation exhibits only a small decrease from the value for perfect order ($= 1$). The autocorrelation of the total CDW modulation $\delta\rho$ decays exponentially with a decay length ~ 4 nm comparable to the inter-impurity spacing $l \approx 5$ nm. Taken together, these facts indicate

that the main effect of the impurity is on the phase of the CDW order parameter.

While all impurities produce a local maximum in the amplitude of the order parameter, different impurities have different consequences for the phase, shown in Fig. 1(c). The main panel shows the phase field corresponding to one component of the CDW. We Fourier transformed the data in Fig. 1(a), and filtered it by retaining only the Fourier component near the six CDW peaks (see the supplementary material for details). The two insets show expanded views of the phase near impurity sites. The right inset shows an impurity that induces a smooth and small phase modulation. The left inset shows that a different impurity induces a large phase modulation from $-\pi$ to π as we move in a counterclockwise fashion around the defect. Only about $\sim 20\%$ of the identifiable defects produce 2π phase modulations (vortices); the remainder produce smoothly varying modulations of the phase. The theoretical analysis presented below suggests that phase slips occur near defects which prefer a phase very different from the average background phase.

To assess the longer length scale effects of impurities, we construct Delaunay loops [18–21, 25] based on the CDW maxima (see the supplementary material). Failure of a loop to close indicates the presence of one or more uncompensated topological defects inside the loop. Fig. 1(b) presents sample loops. While small loops around some impurity sites (broken lines) fail to
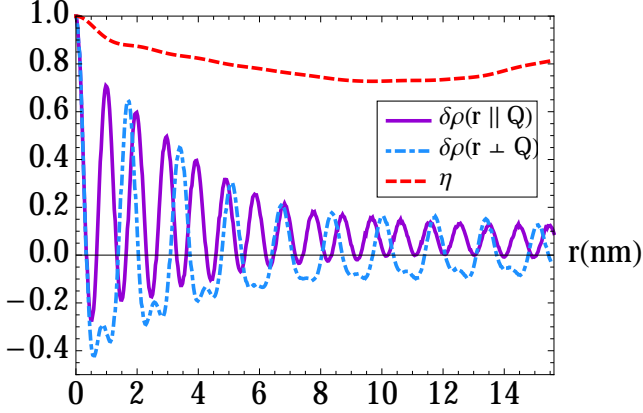
FIG. 2: (Color online) Autocorrelations of the CDW component $\delta\rho$ parallel to and perpendicular to a CDW wave vector $\vec{Q}_1$, and of the amplitudes η.

close, indicating the presence of impurity-induced topological defects, loops of size larger than a few lattice constants (solid lines) do close, indicating that in this field of view dislocations appear only in bound dislocation-antidislocation pairs. The loops continue to close even if the size of the loop becomes as large as the image size, implying that on the length scales accessible to this experiment, there are no free dislocations, in other words that the system is in a Bragg glass phase [4–12], with the decay of the $\delta\rho$ autocorrelation being produced primarily by a smoothly varying phase field, as shown in the main panel of Fig. 1(c).

Thus, in summary, the data presented here indicate that the impurities observed in this NbSe$_2$ sample are strong pinning centers, but nevertheless leave the system in a Bragg glass phase, in apparent disagreement with the conventional idea that the strong impurities induce free topological defects and completely destroy the order [2, 3]. To address the issue we present an energy analysis based on the assumption that the impurities are strong, but also dilute on the scale of the bare CDW coherence length. The analysis is inspired by Refs. 26 and 27, but goes beyond these works by taking into account the long-ranged correlations implied by the fact that the phases obey the Laplace equation.

A crucial issue in the analysis is the dimensionality of the system. While NbSe$_2$ has very anisotropic electronic properties [22], we believe that the appropriate model is three dimensional for the following reasons. First, three dimensional critical scattering is observed in the similar compound $2H-\text{TaSe}_2$ [23], with correlation lengths in the in-plane and out-of-plane directions differing only by a factor of three. Second, below the transition temperature, the development of the order parameter agrees with mean-field theory [23], while a two dimensional in-

commensurate CDW cannot show a true long-range order [28]. Third, a first principles calculation showed that single layer NbSe$_2$ does not exhibit the 3×3 periodicity [29]. These arguments suggest that, most likely because of lattice effect, the CDW in NbSe$_2$ is not unusually anisotropic. In this letter we therefore focus on the three dimensional case, commenting briefly on the differences arising in $d = 2$. More details can be found in the supplementary material.

For simplicity, we consider a CDW described by one phase variable ϕ, and neglect amplitude modulation. We now add impurities at positions x_a; these impurities act to locally pin the phase to the values θ_a. At distances $|\vec{x} - \vec{x}_a| \gg \xi$ (ξ is the coherence length of the CDW) the phase will change; this may take place either by a smooth modulation [as shown in the right inset of Fig. 1(c)] or by creation of a defect-antidefect pair [as shown in the left inset of Fig. 1(c)]. In the absence of defects the free energy of this phase only model is

$$F = \int d^3\vec{x}\rho_S \left(\vec{\nabla}\phi\right)^2 - |V| \sum_a \cos\left[\theta_a - \phi(\vec{x}_a)\right], \quad (2)$$

where ρ_S is the phase stiffness, x_a labels the positions of the impurities, θ_a is the phase energetically favored by the impurity at x_a (this depends on the position of the impurity), and V is the magnitude of the impurity potential [taken to be the same for all impurities in light of the weak variation of amplitudes found in Fig. 1(a)]. We have rescaled lengths by the ratio of in-plane to out of plane coherence lengths. In a simple model, we expect that $\rho_S \sim f_0|\psi|^2\xi_0^2 \sim f_0t\xi_0^2$ with f_0 a measure of the condensation energy per unit volume at $T = 0$, ψ the CDW amplitude, ξ_0 a bare coherence length, and $t = (T_c - T)/T_c$ the reduced temperature, while $V \sim V_0\psi \sim V_0\sqrt{t}$ is proportional to a bare pinning potential V_0 and to the first power of the CDW amplitude. We assume the impurities are dilute (mean inter-impurity distance l much greater than CDW correlation length $\xi = \xi_0/\sqrt{t}$) [30, 31]; this condition breaks down close to the transition temperature, or for dense impurities.

We now consider the energetics of smoothly varying phase configurations, assuming for simplicity that V_0 is very large. At distances larger than a correlation length from any impurity site, minimization of Eq. (2) shows that the phase obeys the Laplace equation $\nabla^2\phi = 0$. So a general solution in the three dimensional case is (for $|\vec{x} - \vec{x}_a| > \xi$)

$$\phi(\vec{x}) = \sum_a \frac{\bar{\theta}_a\xi}{|\vec{x} - \vec{x}_a|}, \quad (3)$$

where $\bar{\theta}_a$'s are parameters to be determined. Substituting this into Eq. (2), we obtain

$$\frac{F}{V} = \frac{\epsilon}{2} \sum_{ab} K_{ab}\bar{\theta}_a\bar{\theta}_b + \frac{1}{2} \sum_a \left(\theta_a - \sum_b K_{ab}\bar{\theta}_b\right)^2. \quad (4)$$
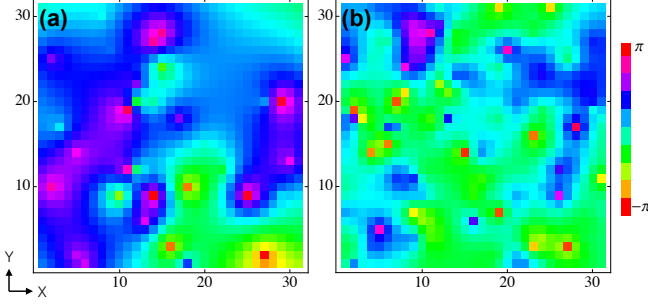
FIG. 3: (Color online) Typical phase configurations obtained from Eq (5) when $\epsilon = 0$ in (a) two dimensions, and (b) three dimensions. The lattice constant is $\xi \sim 1$nm, and the linear system size is 31ξ. The impurity concentration is $n_{\text{imp}} \simeq 0.4\%$.

where the variable inside the parenthesis is taken to be in the range $[-\pi, \pi]$, $\epsilon = 8\pi\rho_S/V$, and I is the identity matrix. The kernel is $K_{ab} = \delta_{ab} + (1 - \delta_{ab})\,\xi/|\vec{x}_a - \vec{x}_b|$. Minimizing Eq. (4) gives

$$\bar{\theta}_a = \sum_b (\epsilon I + K)^{-1}_{ab}\, \theta_b, \qquad (5)$$

The Coulombic form of K means that the inverse matrix $(\epsilon I + K)^{-1}$ has a screening form with a characteristic length $r_{\text{TF}} = \sqrt{l^3(1+\epsilon)/4\pi\xi}$; its Fourier components are

$$(\epsilon I + K)^{-1}(p) = \frac{p^2}{(1+\epsilon)\left(p^2 + r_{\text{TF}}^{-2}\right)}, \qquad (6)$$

Thus, even if the phases θ_a preferred by the impurities are random variables, on scales longer than r_{TF} fluctuations of the $\bar{\theta}$ are suppressed. As a result, the variance $\langle \phi(0)^2 \rangle$ is not infra-red divergent and the solution given in Eq. (5) therefore may have a long ranged order. A further analysis, to be presented in detail elsewhere, shows that the phase fluctuation spectrum is gapped (energy cost of a phase fluctuation of momentum $p \sim p^2 + r_{\text{TF}}^{-2}$). Similar conclusions are found for the two dimensional case, but with a parametrically shorter screening length $r_{\text{TF}} \sim l$ and a more significant effect of defects. There is also a strong dependence of the quantitative results on the short length scale cutoff.

We also numerically solved Eq. (5) when $\epsilon = 0$ on a regular lattice with a lattice constant ξ and $n_{\text{imp}} \simeq 0.4\%$. Fig. 3 shows typical phase configurations in two and three dimensions on a plane (details are presented in the supplementary material). In both cases, the phase varies slowly at long length scales; the two dimensional case, however, has more short length fluctuations (the exact amount depends on the detail of the ultra-violet cut-off).

We now turn to the question of local topological defects. Making a defect on one site a allows the phase to

relax rapidly from the value preferred by the local impurity towards a background value determined by the other defects, decreasing the elastic free energy at the cost of driving the amplitude to zero over a correlation volume. We may estimate that the defect costs an energy $E_{\text{vortex}} \sim f_0 t^2 \xi^3/2 \sim f_0 \sqrt{t}\xi_0^3/2 \sim \rho_S \xi$ with f_0 the zero temperature condensation energy density defined above. The energy gain is associated with removing one defect from the elastic energy. Using the screened Coulombic form of K^{-1} and noting that the θ_a are random variables we obtain that the elastic energy gain is roughly

$$E_{\text{elastic}} \simeq 4\pi\rho_S \xi (1+\epsilon)^{-1}\theta_a^2 + \mathcal{O}(\xi/l). \qquad (7)$$

Thus the energy cost of making a defect-antidefect pair is parametrically equal to the cost of the phase deformation and which one is preferred is determined by an intrinsic property of the CDW [namely the ratio $\kappa = 4\pi\rho_S\xi/E_{\text{vortex}}(1+\epsilon)$] and the square magnitude of the phase deviation caused by the impurity. Our finding that about 20% of impurities induce defects suggests that $\kappa \approx 0.16$, and that defects are only produced when the phase deviates by an amount near its maximal value ($\theta_a \approx \pi$). In $d = 3$ a small finite density of defect loops has no effect on long ranged order, but in $d = 2$ a finite density of vortex/antivortex causes an algebraic decay of correlations (see the supplementary material).

In summary, we have investigated impurity-induced pinning in the CDW state of NbSe$_2$, a paradigm charge density wave state. We find that the impurities are "strong" (enhancing the local CDW amplitude by a factor of two), but both experimental and theoretical analyses show that these impurities lead to a charge density wave phase which varies smoothly over scales parametrically longer than the inter-impurity distance. Only a small fraction of the impurities produce topological defects and these are found to occur only in tightly bound dislocation-antidislocation pairs near the impurities; the material is identified as being in the Bragg glass phase on the scales attainable in the experiment analyzed in this paper. A model analysis shows that dilute but strong impurities give a long-range order, and that the ground state is gapped. The behavior at longer scales and effects of anisotropy are interesting open problems.

* Electronic address: okamoto@phys.columbia.edu

[1] G. Grüner, Rev. Mod. Phys. **60**, 1129 (1988).

[2] H. Fukuyama and P. A. Lee, Phys. Rev. B **17**, 535 (1978).

[3] P. A. Lee and T. M. Rice, Phys. Rev. B **19**, 3970 (1979).

[4] M. V. Feigel'man, V. B. Geshkenbein, A. I. Larkin, and V. M. Vinokur, Phys. Rev. Lett. **63**, 2303 (1989).

[5] T. Nattermann, Phys. Rev. Lett. **64**, 2454 (1990).

[6] J-P. Bouchaud, M. Mezard, and J. S. Yedidia, Phys. Rev. Lett **67**, 3840 (1991).

[7] J-P. Bouchaud, M. Mezard, and J. S. Yedidia, Phys. Rev. B **46**, 14686 (1992).

[8] S. E. Korshunov, Phys. Rev. B **48**, 3969 (1993).

[9] T. Giamarchi and P. Le Doussal, Phys. Rev. Lett. **72**, 1530 (1994).

[10] T. Giamarchi and P. Le Doussal, Phys. Rev. B **52**, 1242 (1995).

[11] T. Giamarchi and P. Le Doussal, Phys. Rev. B **55**, 6577 (1997).

[12] A. Rosso and T. Giamarchi, Phys. Rev. B **70**, 224204 (2004)

[13] E. Sweetland, C-Y. Tsai, B. A. Wintner, J. D. Brock, and R. E. Thorne, Phys. Rev. Lett **65**, 3165 (1990).

[14] S. M. DeLand, G. Mozurkewich, and L. D. Chapman, Phys. Rev. Lett **66**, 2026 (1991).

[15] U. Yaron, P. L. Gammel, D. A. Huse, R. N. Kleiman, C. S. Oglesby, E. Bucher, B Batlogg, D. J. Bishop, K. Mortensen, K. Clausen, C. A. Bolle, and F. De La Cruz, Phys. Rev. Lett. **73**, 2748 (1994).

[16] T. Klein, I. Joumard, S. Blanchard, J. Marcus, R. Cubitt, T. Giamarchi, and P. Le Doussal, Nature **413**, 404 (2001).

[17] S. Ravy, S. Rouzière, J.-P. Pouget, S. Brazovskii, J. Marcus, J.-F. Bérar, and E. Elkaim, Phys. Rev. B **74**, 174102 (2006).

[18] C. A. Murray, P. L. Gammel, D. J. Bishop, D. B. Mitzi, and A. Kapitulnik, Phys. Rev. Lett **64**, 2312 (1990).

[19] D. G. Grier, C. A. Murray, C. A. Bolle, P. L. Gammel, D. J. Bishop, D. B. Mitzi, and A. Kapitulnik, Phys. Rev. Lett **66**, 2270 (1991).

[20] H. Dai and C. M. Lieber, Phys. Rev. Lett. **69**, 1576 (1992).

[21] H. Dai and P. M. Lieber, J. Phys. Chem. **97**, 2362 (1993).

[22] S. V. Dordevic, D. N. Basov, R. C. Dynes, and E. Bucher, Phys. Rev. B **64**, 161103(R) (2001).

[23] D. E. Moncton, J. D. Axe, and F. J. DiSalvo, Phys. Rev. B **16**, 801 (1977).

[24] S. P. Chockalingam, C. J. Arguello, E. P. Rosenthal, L. Zhao, C. Gutiérrez, J. H. Kang, W. C. Chung, R. M. Fernandes, S. Jia, A. J. Millis, R. J. Cava, and A. N. Pasupathy, arXiv:1307.2282 (2013).

[25] P. M. Chaikin and T. C. Lubensky, *Principles of condensed matter physics* (Cambridge University Press, 2000).

[26] S. Abe, J. Phys. Soc. Jpn. **54**, 3494 (1985).

[27] S. Abe, J. Phys. Soc. Jpn. **55**, 1987 (1986).

[28] N. D. Mermin and H. Wagner, Phys. Rev. Lett. **17**, 1133 (1966).

[29] M. Calandra, I. I. Mazin, and F. Mauri, Phys. Rev. B **80**, 241108 (2009).

[30] W. L. McMillan, Phys. Rev. B **16**, 643 (1978).

[31] F. Weber, S. Rosenkranz, J. -P. Castellan, R. Osborn, R. Hott, R. Heid, K. -P. Bohnen, T. Egami, A. H. Said, and D. Reznik, Phys. Rev. Lett **107**, 107403 (2011).